Statistical analysis of plasma filaments in the Wendelstein 7-X stellarator

B. Csillag[1], G. Anda[1], D. Dunai[1], M. Vecsei[1], S. Zoletnik[1], S. Hegedus[1],
C. Killer[2], M. Otte[2], and W7-X Team[2]

[1] *Centre for Energy Research, Budapest, Hungary*

[2] *Max Planck Institute for Plasma Physics, Greifswald, Germany*

Introduction

Blobs or filaments [1] are well known phenomena in tokamaks. These magnetic-field-aligned structures seem to be born near to the separatrix on the low field side of the plasma, and they move radially towards the wall, carrying density with them. Due to the charge separation effect of the curved magnetic field, their radial propagation is driven by the $\underline{E} \times \underline{B}$ drift.

The Wendelstein 7-X stellarator has a complex magnetic topology, and the plasma is bounded by magnetic islands, forming an island divertor. The alkali beam emission spectroscopy (ABES) diagnostic [2] signal is a linear function of the electron density at low density level, thus the fluctuations can be determined with 20 μs time resolution from the SOL through the island until the edge. In the present contribution the properties of plasma filaments in the Wendelstein 7-X stellarator are discussed using conditional averaging techniques and other statistical methods. Comparison between filament behavior in discharges with different magnetic configurations and electron density levels are performed.

Diagnostics

An A-BES diagnostics is installed on Wendelstein 7-X stellarator with a 50 kV sodium beam [2] on the equatorial plane. There is a detector row viewing from the vertical direction through a fibre bundle array, which measures the sodium doublet line intensity ($\sim$ 589 nm) along the beam with 2 MHz sampling rate. The system contains 32 APD and 8 MPPC detectors. Each channel collects light from a 4×0.5 cm (toroidal $\times$ radial) area of the beam. The beam poloidal diameter is 2 cm, thus the diagnostics has reduced sensitivity to perturbations with smaller than 2 cm poloidal size. Fast beam modulation allows beam and background light separation with 20 μs time resolution. In discharges where the beam was slow modulated, the mean background

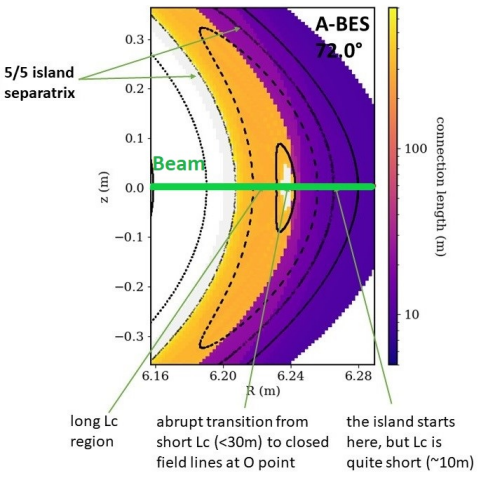

Figure 1: *Connection lengths in standard configuration.*

signal level was substracted from the active signal, then it was integrated to 20 μs time resolution.

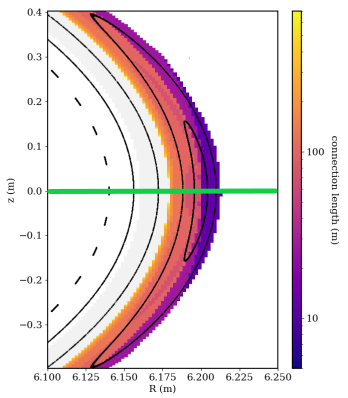

Figure 2: *Connection lengths in high iota configuration.*

Analyzed discharges

Three discharges were analyzed, all of them had $+2.5$ T toroidal field. The first is 20181018.003 with $\iota = 1$ in the divertor island, standard magnetic configuration, 4 MW ECRH, line density $3 \cdot 10^{19} m^{-2}$, and slow sodium beam modulation. Discharge 20180912.014 had $\iota = 1.2$, high iota configuration, 3.47 MW ECRH, line density $2 \cdot 10^{19} m^{-2}$, and here the beam was slow modulated as well. Discharge 20181018.026 had $\iota = 1$, standard configuration, 4.5 MW ECRH, line density $7 \cdot 10^{19} m^{-2}$, and here the beam was fast modulated. Due to the high density, the beam attenuation was significant in the inner side of the island, thus there the measured results are uncertain.

In standard configuration (see Figure 1) on the outer side of the island the connection lengths are around $5 - 15$ m, than at the o-point there are closed field lines. Between the plasma edge and the island o-point the connection lengths are $100 - 1000$ m. But in high iota magnetic configuration the connection length along the beam is similar to a typical tokamak Scrape-Off Layer - plasma edge area, there is a continous transition from a few meter to hundreds, and closed field lines, furthermore the island is narrow - as it can be seen on Figure 2.

Data processing methods

A fast density reconstruction algorithm is available [4] which fits a density profile to the full light profile along the beam. This was found unsuitable for the study of small preturbations as the global fitting introduces non-local response. Thus light signals were used for filament studies. To separate the filaments from other phenomena, like the $0.1 - 1$ kHz fluctuations [5], and because above 10 kHz the spectral density is mostly noise, first order recursive filters were applied in the frequency range of $1.6 - 10$ kHz for statistical moment calculations.

Due to the residual of low frequency oscillations and distortion of temporal signals by the filter a signal level-based conditinal averaging method was found to inadequate. Thus a correlation-based algorithm was developed. Firstly it filters the signal with an $1.6 - 10$ kHz bandpass filter. Secondly it calculates the $C(t)$ correlation between this filtered signal and a filtered Gaussian in a sliding time window. The sign of the Gaussian depends on the sign of the searched events. In the next step the algorithm selects intervals where $C(t) > 3 \cdot \sigma$ (σ is the standard deviation of the correlation), and it slices the unfiltered signals into these intervals. The program executes

that process for different Gaussians with different widths. After that the program calculates the average of the intervals. The interval selection is based on a single signal, but the averaging is done on other detector signals as well, thus the radial filament shape can be determined. A similar method was published [6] with iteration.

Results

Fig. 3 shows statistical properties of the signals at different radial locations. Similar trends can be seen between the statistical moments of low and high density discharges in standard configuration: in the standard deviation profiles there are maxima at o-point, and at the edge, but there is a minimum between them - thus probably there are less filaments in this area. The relative deviation is higher in high density case, which could mean a stronger turbulence. The skewness profiles are also similar at $R > 6.235$ m, and at smaller radial positions there is a difference due to the beam attenuation in the high density case. But overall skewness is close to zero everywhere, thus there should be holes and blobs as well. In high iota configuration high skewness values can be seen, which could mean high positive event rates.

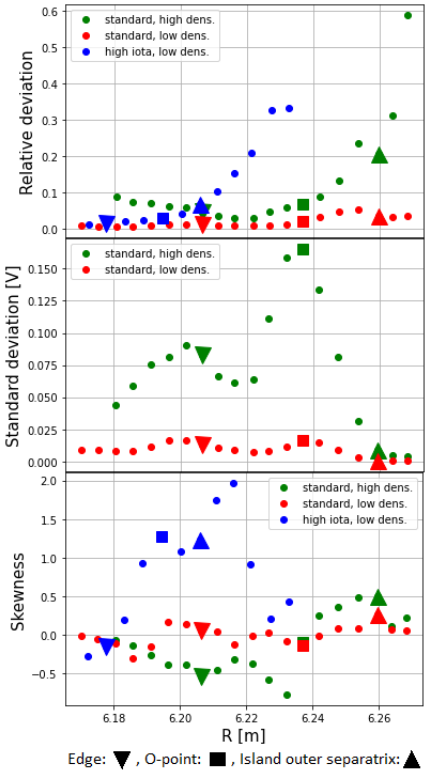

Figure 3: *Statistical moments of the* $1.6 - 10$ *kHz filtered signals.*

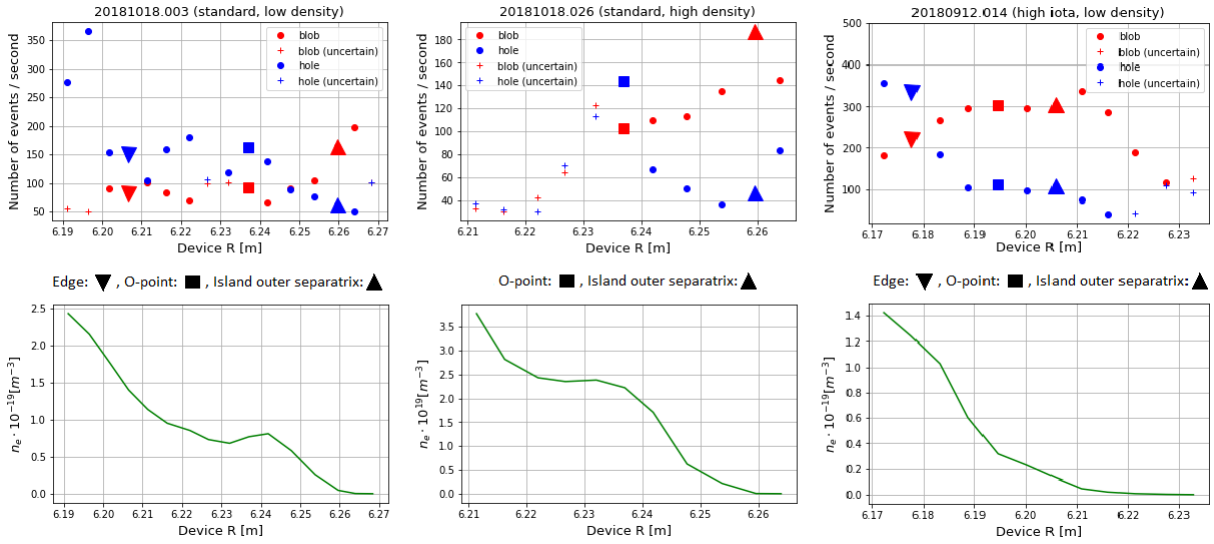

Figure 4: *Filament rate profiles from conditional averaging results in different configurations.*

On Figure 4 in standard configuration, at low density many holes can be seen inside the edge, and there are dominantly holes on the inboard side of the island. On the outboard side of the island blobs dominate. The high density case is similar here as well (but there are less useful data due to the beam attenuation), although there this blob-dominated area begins deeper in the island. Filaments disappear around $R = 6.225\ m$, where the standard deviation profiles have a minimum. In high iota configuration the whole rate profile is similar to the tokamak case. Fig. 5. shows the results of the 2D conditional averaging. The interval selection was done at the radius indicated by the dashed line. There is a connection between events at the outer side of the island, and at the edge, as it was observed before in correlations [3].

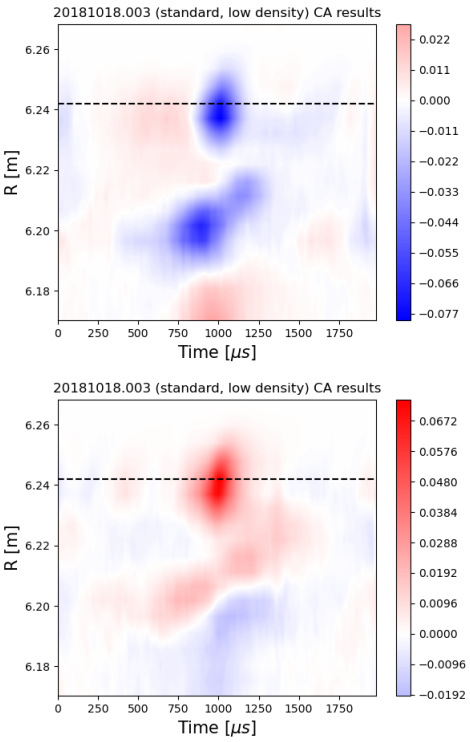

Figure 5: *2D CA results for discharge* 20181018.003.

Summary

In the standard configuration the statistical moments and event rate profiles are similar at high and low density, although the deviations grow with the density. There is a connection between events at the edge, and the outer side of the island. In high iota configuration the statistical properties and the event rates are similar to filaments measured on tokamaks (in contrast to standard configuration results, and Langmuir probe measurement results [7] in low iota), probably because in this case the magnetic structure is similar as well.

Acknowledgement

This work was carried out within the framework of the EUROfusion Consortium and has received funding from the Euratom research and training programme 2014–2018 and 2019–2020 under grant agreement No 633053. The views and opinions expressed herein do not necessarily reflect those of the European Commission.

References

[1] D'Ippolito D A, *et al*, Physics of Plasmas **18** 060501 (2011)

[2] S. Zoletnik *et al* Review of Scientific Instruments **89**, 10D107 (2018).

[3] S. Zoletnik *et al* Plasma Physics and Controlled Fusion **62**, 014017 (2020).

[4] M. Vécsei, *et al*, 46th EPS Conference on Plasma Physics P4.1021 (2019)

[5] Ballinger S B, *et al*, Nuclear Materials and Energy **17** 269 (2018)

[6] F Kin, *et al*, Plasma and Fusion Research: **14** 1402114 (2019)

[7] C. Killer *et al* Plasma Physics and Controlled Fusion **62**, 085003 (2020).